Dalton Transactions

Accepted Manuscript

This is an *Accepted Manuscript*, which has been through the Royal Society of Chemistry peer review process and has been accepted for publication.

Accepted Manuscripts are published online shortly after acceptance, before technical editing, formatting and proof reading. Using this free service, authors can make their results available to the community, in citable form, before we publish the edited article. We will replace this *Accepted Manuscript* with the edited and formatted *Advance Article* as soon as it is available.

You can find more information about *Accepted Manuscripts* in the Information for Authors.

Please note that technical editing may introduce minor changes to the text and/or graphics, which may alter content. The journal's standard Terms & Conditions and the Ethical guidelines still apply. In no event shall the Royal Society of Chemistry be held responsible for any errors or omissions in this *Accepted Manuscript* or any consequences arising from the use of any information it contains.

ROYAL SOCIETY OF CHEMISTRY

www.rsc.org/dalton

Journal Name RSCPublishing

ARTICLE

Cite this: DOI: 10.1039/x0xx00000x

Received 00th January 2012,
Accepted 00th January 2012

DOI: 10.1039/x0xx00000x

www.rsc.org/

Distinctive EPR signals provide understanding of the affinity of *bis*-(3-hydroxy-4-pyridinonato) copper (II) complexes for hydrophobic environments

Maria Rangel[a*], Andreia Leite[b], André M. N. Silva[b], Tânia Moniz[b], Ana Nunes[b], M. João Amorim[b], Carla Queirós[b], Luís Cunha-Silva[b], Paula Gameiro[b], and John Burgess[c],

In this work we report the synthesis and characterization of a set of 3-hydroxy-4-pyridinone copper(II) complexes with variable lipophilicity. EPR spectroscopy was used to characterize the structure of copper(II) complexes in solution, and as a tool to gain insight into solvent interactions. EPR spectra of solutions of the [CuL_2] complexes recorded in different solvents reveal the presence of two copper species whose ratio depends on the nature of the solvent. Investigation of EPR spectra in the pure solvents methanol, dimethylsulfoxide, dichloromethane and their 50% (V:V) mixtures with toluene, allowed the characterization of two types of copper signals (g_{zz}=2.30 and g_{zz}=2.26) whose Spin-Hamiltonian parameters are consistent with solvated and non-solvated square-planar copper(II) complexes. Regarding the potential biological application of ligands and complexes, and to get insight on partition properties in water/membrane interfaces, EPR spectra were also obtained in water-saturated octanol, an aqueous solution buffered at pH=7.4 and liposome suspensions, for three compounds representative of different hydro-lipophilic balances. Analysis of the EPR spectra obtained in liposomes allowed establishment of the location of the complexes in the water and lipid phases.
In view of the results of this work we put forward the use of EPR spectroscopy to assess the affinity of the copper(II) complexes for a hydrophobic environment and also to obtain indirect information about the lipophilicity of the ligands and similar EPR silent complexes.

Introduction

Ligands of the 3-hydroxy-4-pyridinone (3,4-HPO) type are well known, mainly by reason of their biomedical applications.[1-10] 3-hydroxy-4-pyridinones are particularly attractive for pharmaceutical purposes since their structure allows tailoring of their hydrophilic/lipophilic balance (HLB) without significantly altering the stability constants for a particular metal ion. The 3-hydroxy-4-pyridinone ligands are synthesized by the reaction of 3-hydroxy-4-pyrones with primary amines and variations in HLB can be achieved by introducing appropriate substituents on the endocyclic nitrogen atom of the pyridinone ring by choosing the appropriate amine, thus leading to the optimal lipophilicity for delivery to, or removal of metal ions from, the human body.
Although 3,4-HPO ligands are better known as iron chelators, which have been successfully used in the treatment of iron overload disorders, their potential use in the regulation of copper homeostasis seems plausible to consider. An excess of copper is the main trait in Wilson's disease and copper accumulation in the brain has been associated with the pathology of neurodegenerative disorders such as Alzheimer's and Parkinson's diseases.[11-14] Furthermore, an insulin-like effect has been identified for copper(II) and copper chelators have proved to be suitable carriers for the metal ion.[15]

Dalton Transactions Accepted Manuscript

Table 1: Formulae and abbreviations for ligands and of copper(II) complexes.

Ligand formula	Substituents		Ligand abbreviation	Complex formula	Complex Abbreviation
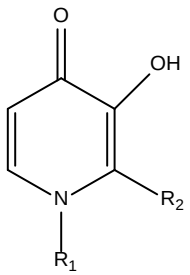	R_1 = H	R_2 = CH_3	Hmpp	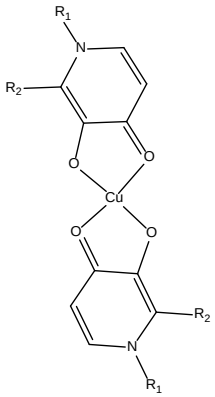	1 - Cu(mpp)$_2$
	R_1 = CH_3	R_2 = CH_3	Hdmpp		2 - Cu(dmpp)$_2$
	R_1 = CH_2CH_3	R_2 = CH_3	Hmepp		3 - Cu(mepp)$_2$
	R_1 = CH_3	R_2 = CH_2CH_3	Hempp		4 - Cu(empp)$_2$
	R_1 = CH_2CH_3	R_2 = CH_2CH_3	Hdepp		**5 - Cu(depp)$_2$**
	R_1 = $(CH_2)_2OH$	R_2 = CH_3	Hhempp		6 - Cu(hempp)$_2$
	R_1 = $(CH_2)_2OH$	R_2 = CH_2CH_3	Hheepp		**7 - Cu(heepp)$_2$**
	R_1 = $(CH_2)_5CH_3$	R_2 = CH_3	Hhexylmpp		**8 - Cu(hexylmpp)$_2$**

In order to appraise the possible use of 3,4-HPO ligands either for copper removal or delivery, information on stability constants, speciation in aqueous solution and lipophilicity of the copper complexes is required. The values of stability constants provide information about the ligand selectivity for copper(II) and possible competition with other metal ions present in the biological milieu and allow comparison of the predominant species in solution for a certain pH value or metal:ligand ratio. Knowledge regarding lipophilicity allows a rational selection of the ligand which will be more appropriate to carry the copper ion across biological membranes.

In the present paper we report on the synthesis and speciation in aqueous solution of a set of 3,4-HPO copper(II) complexes with variable lipophilicity (Table 1). Electron Paramagnetic Resonance spectroscopy was used to characterize the structure of the copper(II) complexes in solution, and as a tool to gain insight into complex-solvent interactions.

Experimental

Materials

Reagents and solvents were purchased as reagent-grade and used without further purification unless otherwise stated. The 3-hydroxy-4-pyridinone ligands were synthesized and purified as previously described.[16] Mass spectra were obtained by "Unidade De Espectrometria De Masas de Santiago de Compostela" and microanalyses were obtained by "Unidad De Análisis Elemental of Santiago de Compostela".

Methods

Synthesis

Ligands were prepared in our laboratory according to the methods previously described.[16] The corresponding copper (II) complexes, whose formulae and abbreviations are shown in Table 1, were synthesized following the method described by Gerard and by us[16, 17], which is based on the reaction of the ligand with the metal ion salt in aqueous or aqueous/organic solution depending on the lipophilicity of the ligand. In order to avoid the concomitant formation of metal ion hydroxides a 1:2.2 metal-to-ligand ratio was used and ligand deprotonation was performed prior to solution mixture by raising to 9 the pH of the solution containing the ligand. The appropriate pyridinone (22 mmol) was dissolved in water and sodium hydroxide (NaOH) (20 mmol) was added. The solution was stirred for 10 min followed by addition of 10 mmol of copper nitrate dissolved in the minimum amount of water. Formation of the complexes begins after reagent mixing and the solution is left under agitation overnight to maximize the yield. The green solids obtained were filtered, washed with the minimum amount of cold water, transferred to a desiccator containing P_2O_5 and after 2 days dried under vacuum for further 72 h. The water content found in the complexes was checked by the Karl Fischer method. The copper (II) complexes were isolated in the solid state as green powders and characterized by elemental analysis and mass spectra obtained by Fast Atom Bombardment (FAB-MS) or Matrix-assisted laser desorption/ionization (MALDI), which exhibited the peaks of the molecular ion $[M^+ H]^+$. For complex [Cu(hexylmpp)$_2$], (nº 8 in Table 1), recrystallization from methanol resulted in the formation of crystals suitable for single-crystal X-ray diffraction studies, which allowed the crystal structure determination.

Bis(3-hydroxy-2-methyl-4-pyridinonato)copper(II), Cu(mpp)$_2$. $C_{12}H_{12}N_2O_4Cu.0.5\ H_2O$: found: C, 44.89; H, 4.05; N, 8.70; calcd. C, 44.93; H, 4.08; N, 8.73; FAB-MS m/z 312 $[M+H]^+$;

Dalton Transactions Accepted Manuscript

This journal is © The Royal Society of Chemistry 2012

Bis(1-ethyl-3-hydroxy-2-methyl-4-pyridinonato)copper(II), Cu(mepp)$_2$. $C_{16}H_{20}N_2O_4Cu$: found: C, 52.06; H, 5.40; N, 7.59, calcd.: C, 52.19 ; H, 5.44; N, 7.61, FAB-MS: m/z 368 $[M+H]^+$;
Bis(2-ethyl-3-hydroxy-1-methyl-4-pyridinonato)copper(II), Cu(empp)$_2$. $C_{16}H_{20}N_2O_4Cu$: found: C, 52.25; H, 5.49; N, 7.69, calc.: C, 52.19; H, 5.44; N, 7.61; FAB-MS: m/z 368 $[M+H]^+$.
Bis(1,2-dimethyl-3-hydroxy-4-pyridinonato)copper(II), Cu(dmpp)$_2$. $C_{14}H_{16}N_2O_4Cu$: found: C, 49.48; H, 4.75; N, 8.24, calcd.: C, 49.44; H, 4.75; N, 8.18, FAB-MS: m/z 340 $[M+H]^+$;
Bis(1,2-diethyl-3-hydroxy-4-pyridinonato)copper(II), Cu(depp)$_2$. $C_{18}H_{24}N_2O_4Cu$: found: C, 54.40; H, 6.01; N, 7.01, calcd.: C, 54.60; H, 6.11; N, 7.07, FAB-MS: m/z 396 $[M+H]^+$.
Bis(3-hydroxy-1-(2-hydroxyethyl-2-methyl-4-pyridinonato)copper(II), Cu(hempp)$_2$. $C_{16}H_{20}N_2O_6Cu.3/2\ H_2O$: found: C, 44.38; H, 5.38; N, 6.54, calcd.: C, 45.01; H, 5.43; N, 6.56; FAB-MS m/z: 400 $[M+H]^+$;
Bis(3-hydroxy-1-(2-hydroxyethyl-2-ethyl-4-pyridinonato) copper(II), Cu(heepp)$_2$. $C_{18}H_{24}N_2O_6Cu$: found: C, 50.64; H, 5.69; N, 6.54, calcd.: C, 50.52; H, 5.65; N, 6.55; FAB-MS m/z: 428 $[M+H]^+$.
Bis(3-hydroxy-2-methyl-1-hexyl-4-pyridinonato) copper(II), Cu(hexylmpp)$_2$. $C_{24}H_{32}N_2O_4Cu$: found: C, 59.90; H, 7.33; N, 5.80, calcd.: Cu: C, 60.04; H, 7.56; N, 5.83; FAB-MS m/z: 480 $[M+H]^+$.

Single-crystal X-Ray diffraction

Crystalline material of the complex [Cu(hexylmpp)$_2$] was manually harvested, and a suitable single crystal was mounted on a glass fiber using FOMBLIN Y perfluoropolyether vacuum oil (LVAC 25/6), with the assistance of a stereomicroscope.[18] Diffraction data acquisition was performed with a Bruker X8 Kappa APEX II Charge-Coupled Device (CCD) area-detector diffractometer: Mo Kα graphite-monochromated radiation, λ = 0.71073 Å; the crystal was positioned at 35 mm from the detector and a 10 s exposure was used, with the collection controlled by the APEX2 software package.[19] The temperature of acquisition (150 K) was set up with a cryosystem by the Oxford Cryosystems Series 700 monitored by the interface Cryopad.[20] Images were processed in the software SAINT$^+$,[21]and absorption was corrected using the multi-scan semi-empirical method implemented in SADABS.[22]
The structure was solved by direct methods implemented in SHELXS-97,[23, 24] allowing the immediate identification of the Cu atom, with the remaining non-hydrogen atoms located from difference Fourier maps calculated by successive full-matrix least-squares refinement cycles on F2 using SHELXL-97,[23, 24] and were successfully refined with anisotropic displacement parameters.
The alkyl chain of one of the ligands of the complex shows some positional disorder, particularly clear in the last three C-atoms (C22, C23 and C24). However the limited quality of the diffraction data prevented a rational modelling of this disorder. Several further attempts that were performed resulted in unrealistic molecular geometries of the alkyl chain. Although the impossibility of modelling the disorder in a reasonable structural arrangement, the problems in the molecular geometry were minimized with additional refinement cycles using suitable restrains such as DFIX and ISOR.
H-atoms bonded to C-atoms of the ligand were located at their idealized positions using appropriate HFIX instructions in SHELXL: 43 for the aromatic Hs, 23 for the $-CH_2-$ groups and 137 for terminal $-CH_3$ groups. The latter were included in subsequent refinement cycles in riding-motion approximation with isotropic thermal displacements parameters (Uiso) fixed at 1.2 × Ueq (for the aromatic and CH_2 groups) and 1.5 × Ueq (for the methyl group) of the carbon atom to which they are attached. The last difference Fourier map synthesis revealed the highest peak (1.27 eÅ−3) and deepest hole (−0.63 eÅ−3) located at 0.74 Å and 0.75 Å from C24, respectively.
Information concerning crystallographic data collection and structure refinement details is summarized in Table 2. Crystallographic data (excluding structure factors) have been deposited with the Cambridge Crystallographic Data Centre as supplementary publication no. CCDC-970589 Copies of the data can be obtained free of charge on application to CCDC, 12 Union Road, Cambridge CB2 2EZ, U.K (FAX: +44 1223 336033), or online via www.ccdc.cam.ac.uk/data_request/cif or by emailing data_request@ccdc.cam.ac.uk.

Potentiometric measurements

All solutions were prepared with doubly de-ionized water (conductivity less than 0.1 μS cm^{-1}). Solutions of NaOH were prepared in de-ionized water previously purged with argon while boiling to minimize carbonate impurity. Potentiometric measurements were performed with a Crison 2002 decimilivoltimeter and a Crison 2031 automatic burette controlled by computer. The electrode assembly consisted of a Russell 900029/4 double junction Ag/AgCl reference electrode and a Russell 18026/02 glass electrode as indicator. All titrations were carried out in a thermostat-controlled double-walled glass cell at (25.0±0.1) ºC under argon atmosphere, solution homogeneity was maintained by agitation using a Crison 2038 magnetic agitator and ionic strength was adjusted to 0.10 M with NaCl. System calibration was performed by the Gran method[25] in terms of hydrogen ion concentration by titrating solutions of strong acid with strong base. Before each run a calibration was performed to check the electrode behavior. Stock solutions of 3-hydroxy-4-pyridinones (1.0×10^{-2} M) were prepared in water (I=0.1 M NaCl). The determination of the stability constants of the binary complexes was performed by titration of H^+(aq) (1.0-2.0 mM, I= 0.1 M NaCl, 25.0 ºC) in the presence of copper salt (2.0 mM) and the 3-hydroxy-4-pyridinone ligands (2.0-6.0 mM) with NaOH (*ca.* 3.0×10^{-2} M) under argon atmosphere. The stability constants were determined from the results of experiments in which 1:1, 1:2 and 1:3 metal/ligand ratios were used, and each titration was performed 5 times to check the reproducibility of the data.
The global equilibrium constants defined by Eqs. (1) and (2):

$$p\mathrm{M} + q\mathrm{L} + r\mathrm{H} \leftrightarrows M_pL_qH_r \qquad (1)$$

Dalton Transactions Accepted Manuscript

$$\beta_{pqr} = \left[M_p L_q H_r\right]^{2p-q+r} \Big/ [M]^p [L]^q [H]^r \qquad (2)$$

(where M is the metal, L the 3,4-HPO in its anionic form, H^+ the proton and p, q, r the stoichiometric coefficients) were refined by least-squares calculation using the computer program Hyperquad[26] taking into account the presence of the hydroxide species of copper and the protolysis of water. The errors associated to the *βpqr* values were determined using the Albert and Sergeant theory.[27]

Liposome preparation. Liposomes were prepared by evaporating a lipid solution of dimyristoylphosphatidylcholine (DMPC) in chloroform to dryness with a stream of argon. The films were left under vacuum for a minimum of three hours to remove all traces of the organic solvent. The resulting dried lipid films were dispersed with 10 mM 3-(N-morpholino)propanesulfonic acid (MOPS) buffer (0.1 M NaCl, pH 7.4), and the mixture was vortexed above the phase transition temperature (310 K) to produce multilamellar liposomes (MLV). After this, the MLV were submitted five times to the following cycle: the vesicles were frozen in liquid nitrogen and the sample was thawed in a water bath at 37 ºC. Lipid suspensions were equilibrated at 37 ºC for 30 min and extruded ten times through polycarbonate filters (100 nm) in order to produce large unilamellar vesicles (LUVs).

Electron paramagnetic resonance

The samples were prepared by dissolution of the compound in the appropriate solvent and transferred to a capillary tube which was placed in the EPR quartz tube. EPR spectra were recorded at RT and in frozen solution using an X-band (9 GHz) Bruker ELEXSYS E 500 spectrometer equipped with a variable temperature unit (ER 4B1 VT), available at Laboratório de Ressonância Paramagnética Electrónica, (Centro de Materiais da Universidade do Porto) and obtained in the following general experimental conditions: microwave frequency of 100 kHz, microwave power of 20 mW, modulation amplitude of 8 G, gain 60 dB, acquisition time of 600s, at (100 ± 1) K. The spectra were simulated with the computer suite program Bruker WinEPR/SimFonia.

Results and Discussion

The results obtained for the synthesis and characterization of the complexes confirmed that the method described by Gerard[17] is also appropriate for the synthesis of 3,4-HPO copper complexes as previously observed for the corresponding Zn(II), Ni(II) and Co(II) compounds.[16]

Structure description of [Cu(hexylmpp)$_2$]: the formation of the *bis* chelate complex was unequivocally demonstrated by the crystal structure of the Cu complex with the ligand Hhexylmpp. Single-crystals suitable for X-ray diffraction (XRD) analysis were isolated by controlled recrystallization from methanol. Unfortunately, the several attempts and distinct procedures performed to obtain single-crystals of the other complexes appropriate for XRD analysis was unsuccessful. Interestingly, searches in the literature and in the Cambridge Structural Database (CSD, Version 5.33 2012, with two updates)[28, 29] reveal that despite the large number of studies involving Cu(II) compounds with pyridinone-based ligands the number of crystal structures of *bis* chelate complexes is very small.[30-33]

The crystal structure of the complex Cu(hexylmpp)$_2$ was determined in the trigonal space group R-3, with the asymmetric unit comprising one neutral complex entity, without any solvent molecule (Figure 1, Table 2).

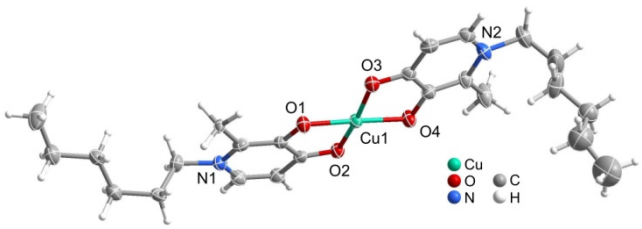

Figure 1. Crystal structure of the copper(II) complex Cu(hexylmpp)2, showing the labelling scheme for the metal coordination centre and N-atoms. All non H elements are represented as ellipsoids (drawn at 50% probability level) and H atoms as arbitrary spheres.

Table 2: Crystal and structure refinement data for the complex [Cu(hexylmpp)$_2$]

Formula	$C_{24}H_{36}N_2O_4Cu$
Mr	480.10
Crystal morphology	Prism green
Crystal size /mm	0.25 × 0.16 × 0.10
Crystal system	Trigonal
Space group	R-3
a /Å	27.206(5)
b /Å	27.206(5)
c /Å	16.478(2)
α /°	90
β /°	90
γ /°	120
Volume /Å^3	10563(3)
Z	18
ρcalculated /g cm^{-3}	1.359
F(000)	4590
μ /mm^{-1}	0.962
θ range /°	3.67 to 25.02
Index ranges	$-30 \le h \le 31$ $-32 \le k \le 32$ $-14 \le l \le 19$

Dalton Transactions Accepted Manuscript

This journal is © The Royal Society of Chemistry 2012

Reflections collected	16219
Independent reflections	4040 (R_{int} = 0.0562)
Final R indices [I>2σ(I)]	R1 = 0.0516; wR2 = 0.1374
Final R indices (all data)	R1 = 0.0758; wR2 = 0.1491
Largest diff. peak and hole /e Å^3	1.272 and −0.632

The Cu(II) centre coordinated to two pyridinone rings, with the two keto- oxygen atoms and the two phenolic oxygen atoms in *trans* orientation to each other, ultimately originating a slightly distorted square-planar coordination geometry. This coordination mode of the two pyridinone ligands is analogous to that of other copper(II)-pyridinonato complexes previously reported, with the *cis* angles O–Cu–O ranging from 86.13(9) to 94.56(9)º and the two angles trans are 163.35(9) and 171.69(9)º.[30-33] The distances between the oxygen atoms and the copper centre are also similar to those found in similar complexes: the bond lengths between the keto- oxygen atoms (O2 and O3) and the metal are 1.933(2) and 1.930(2) Å, respectively, while those involving the phenolic oxygen atoms (O1 and O4) are smaller, 1.908(2) and 1.917(2) Å.

The neighbouring complexes interact by a number of weak intermolecular C–H···O hydrogen bonds and C–H···π type interactions and donor groups available to form strong hydrogen bonds (Figure 2a; Table 3 summarize the main geometrical details of the most relevant and chemically feasible weak hydrogen bonds). In the C–H···O interactions, the H···O distances range from 2.419(3) to 2.705(3) Å, while the C-H-O angles are found between 117(2) and 170(2)º. As mentioned, in addition to the weak C–H···O hydrogen bonds, there is also one type of intermolecular C–H···π interaction (C2–H2···Cg, with H···Cg distance of 2.909(1) Å and C-H-Cg angle of 153(1)º; Cg represents the centroid of the aromatic ring formed by C13, C14, C15, C16, C17 and N2), leading to a supramolecular network. As a consequence of this supramolecular network of weak intermolecular interactions and the arrangement of the alkylic chains of the ligand, the extended crystal packing reveals hydrophobic channels running in the [110] direction of the unit cell (Figure 2b). Interestingly, these circular channels (internal diameter in the range 5-6 Å) results from the arrangement of the alkylic chains in a shape like the "Star of David" (Figure 2c).

Table 3: Geometric information (distances in Å and angles in degrees) for the C–H···O interactions of the [Cu(hexylmpp)$_2$] crystal structure.

C–H···O	d (H···A)	d (D···A)	∠ (DHA)
C1–H1···O4^{i}	2.687(2)	3.566(4)	152(2)
C6–H6B···O1^{ii}	2.509(2)	3.435(4)	158(2)
C7–H7A···O4^{i}	2.705(2)	3.652(4)	160(2)
C8–H8B···O2^{i}	2.505(3)	3.266(5)	134(2)
C9–H9B···O3^{ii}	2.653(2)	3.223(3)	117(2)
C18–H18B···O4^{ii}	2.545(2)	3.301(4)	134(2)
C19–H19A···O2^{ii}	2.500(2)	3.451(4)	161(2)
C19–H19B···O3^{iii}	2.419(3)	3.391(6)	167(3)
C21–H21B···O1^{iii}	2.674(3)	3.652(9)	170(4)

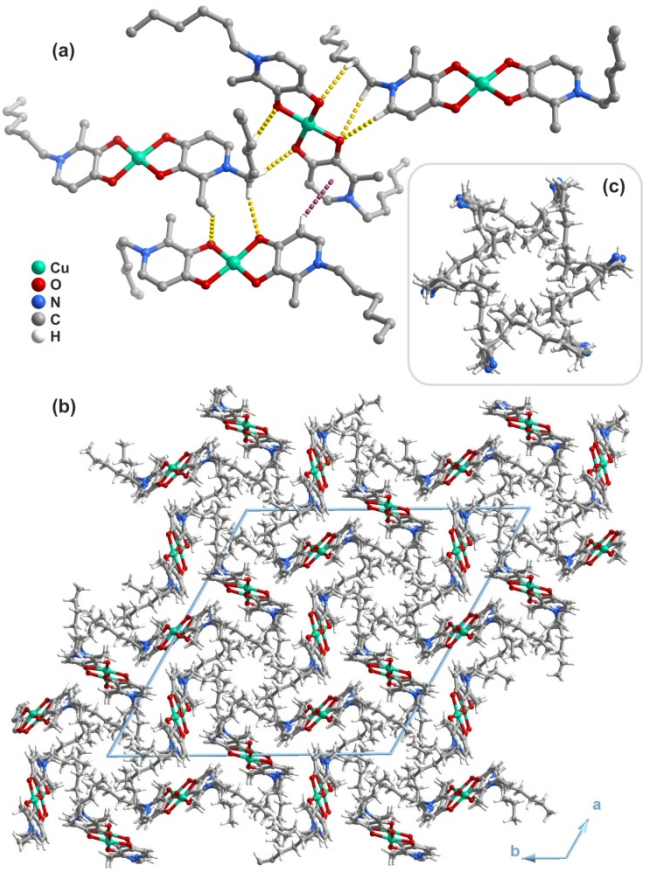

Figure 2. (a) C–H···O and C–H···π interactions involving three adjacent complexes; these intermolecular interactions are represented as yellow and violet dashed lines, respectively, and only the H-atoms involved directly in C–H···O and C–H···π interactions are represented. (b) Crystal packing viewed in the [0 0 1] direction of the unit cell. (c) A circular channel that results of the arrangement of the alkylic chains in a shape like the "Star of David" (internal diameter in the range 5-6 Å).

Dalton Transactions Accepted Manuscript

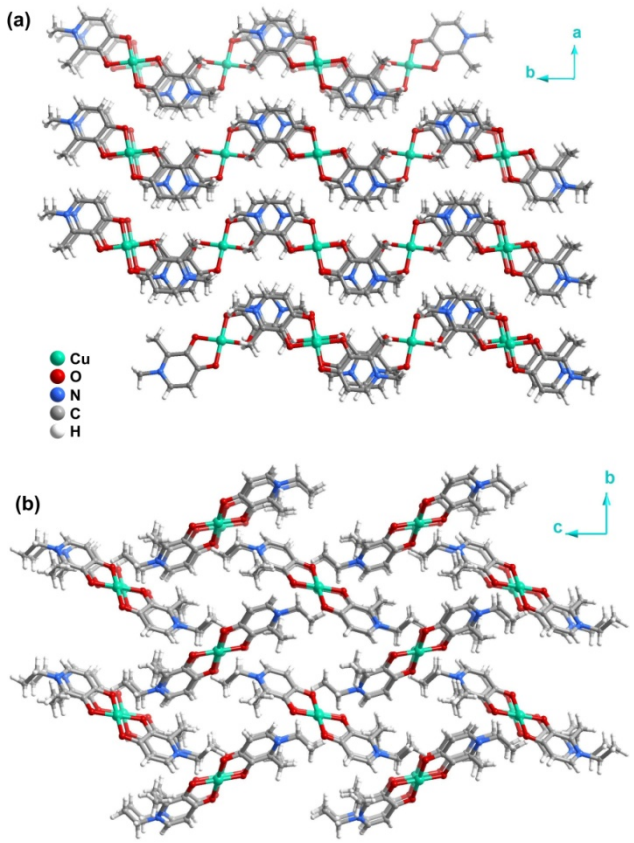

Figure 3. Crystal packing of (a) *bis*(1,2-dimethyl-3-hydroxy-4-pyridinonato)copper(II) complex, [Cu(dmpp)$_2$], viewed in the [0 0 1] direction of the unit cell and (b) *bis*(1,2-diethyl-3-hydroxy-4-pyridinonato)copper(II) complex, [Cu(depp)$_2$], viewed in the [1 0 0] direction of the unit cell. Figures were prepared from the respective CIF files deposited in the CDS database with the codes WELTEM and WELTOM.

Aqueous solution studies

The stability constants of the copper(II) 3-hydroxy-4-pyridinone complexes were determined by potenciometry and are recorded in Table 4. We have previously reported the acidity constants of the ligands, pK_a.[16]

Table 4: Values of the stability constants of the copper (II) complexes with the 3,4-HPO ligands, T = 25ºC and I = 0.1 M NaCl.

Ligand	logβ_{110}	logβ_{120}	logK_2
Hmpp	9.78±0.04	18.16±0.1	8.38
Hdmpp	10.21±0.03	18.66±0.04	8.45
Hempp	9.90±0.03	17.85±0.04	7.95
Hmepp	9.53±0.04	17.18±0.03	7.65
Hdepp	9.70±0.03	17.50±0.05	7.80
Hhempp	10.30±0.04	19.00±0.04	8.70
Hheepp	10.00±0.04	18.50±0.04	8.50

The values of the acidity constants of the ligands, metal ion and water protolysis constants, in the experimental conditions adopted in this study, were used as fixed parameters in the refinement of data regarding the metal–ligand systems in accordance with the proposed model Equations (3), (4) and (5).

$$M^{2+}(aq) + L^{-}(aq) \rightleftarrows [ML]^{+}(aq) \log\beta_{110} \quad (3)$$

$$M^{2+}(aq) + 2L^{-}(aq) \rightleftarrows [ML_2](aq) \log\beta_{120} \quad (4)$$

$$M^{2+}(aq) + 3L^{-}(aq) \rightleftarrows [ML_3]^{-}(aq) \log\beta_{130} \quad (5)$$

Due to the low water solubility of ligand 8, under the experimental conditions adopted, the stability constants could not be determined for the corresponding copper complex. In order to allow the possible formation of CuL_3 species, the affinity of the various ligands towards copper (II) was evaluated by studying the interaction of the metal ion with the ligands in solutions containing 1:1, 1:2 and 1:3 metal:ligand ratios using a concentration of Cu^{2+} equal to $2x10^{-3}$ M.

The values of the stability constants obtained in this work are similar for all the ligands. Comparing the values obtained for the copper(II) complexes with those of other divalent metal ions with the same ligands it is possible to observe that the copper(II) stability constants are *ca* 10^5 times greater than those of zinc(II)[5], *ca* 10^7 times greater than those nickel(II) and cobalt(II)[16] and *ca* 10^3 times smaller than those of oxovanadium(IV)[34]. The values follow the Irving–Williams series ($Co^{2+}<Ni^{2+}<Cu^{2+}>Zn^{2+}$) thus providing additional evidence for similar coordination geometry in solution. Speciation diagrams have been calculated for the different ligands in the conditions specified in Figure 4 for the ligand Hdepp.

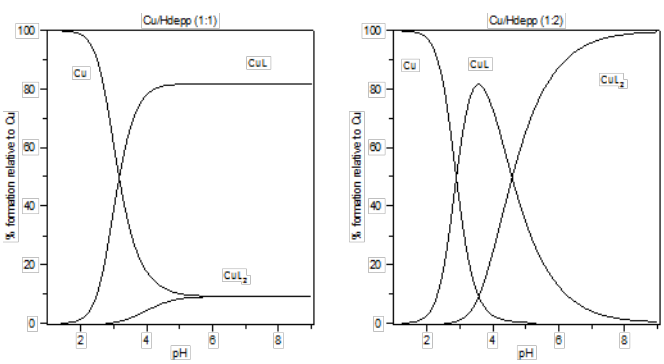

Figure 4 - Speciation diagrams for the Cu^{2+}/Hdepp system with 1:1 and 1:2 metal/ligand molar ratios and a metal concentration of 2 mM.

The diagrams show that complex formation starts at very acidic pH values and that for pH > 5, in both metal/ligand molar ratios, the predominant species are Cu(II) complexes thus

Dalton Transactions Accepted Manuscript

This journal is © The Royal Society of Chemistry 2012

suggesting that these ligands have a strong affinity for Cu(II). The speciation diagrams also indicate that at physiological pH values the major complex species is, [CuL] for 1:1 ratio and [CuL_2] for 1:2 ratio.

In order to validate the set of equilibria used in the potentiometric determinations and the speciation diagrams EPR spectra of solutions of Cu^{2+} and ligand in 1:1 and 1:2 molar ratios obtained at different pH values. A representative set of spectra is displayed in Figure 5.

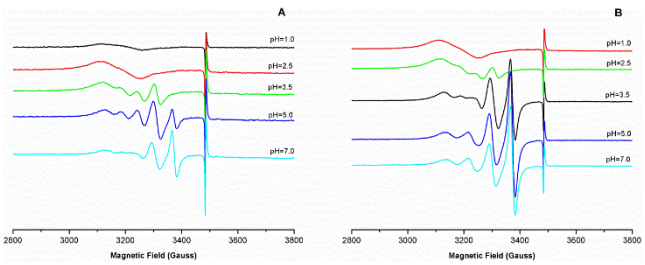

Figure 5- EPR spectra of the Cu^{2+}/Hdepp system with 1:1 (A) and 1:2 (B) metal/ligand molar ratios and a metal concentration of 2 mM.

The two sets of EPR spectra obtained and depicted in Figure 5 validate the model used for the stability constants calculation and speciation diagrams. Spectra show that for pH values >2.5 more than one copper (II) species is present in solution. For the 1:1 metal/ligand molar ratio at pH below 2.5 only one species can be detected while for 1:1 metal/ligand molar ratio features of a complex can be seen. Analyzing the speciation diagrams, in Figure 4, it can be seen that for the metal/ligand molar ratio 1:1 at pH=2.5 90% of copper(II) present in solution is in the Cu^{2+}(aq) form and 10% in the [CuL] form, whereas for the metal/ligand molar ratio 1:2, 80% of copper(II) is in the Cu^{2+}(aq) form and 20% is in the [CuL] form. This difference allows the EPR detection, at pH=2.5, of the [CuL] form in the 1:2 metal/ligand molar ratio.

EPR studies in various solvents and liposome suspensions

In order to obtain structural insight into the copper coordination sphere, EPR spectra were obtained in methanol at 100 K for all the copper(II) complexes under study. The spectra are identical for the various complexes and in Figure 6 the spectrum of compound 8 is depicted.

The spectrum exhibits main features characteristic of an interaction of an unpaired electron (S=1/2) with the copper nuclei ($^{65}Cu/^{63}Cu$, I=3/2) and is similar to those described for square-planar copper(II) complexes with tetragonal distortions and a $^2B_1$ ($d(x^2-y^2)$) ground state.[35-38]. Spectral anisotropy allows for the hyperfine splitting, derived from the electron spin interaction with the copper nucleus spin ($^{65}Cu/^{63}Cu$, I=3/2), to be particularly well resolved in the lowest magnetic field region of the spectra.[36, 38] This hyperfine interaction gives rise to 5 lines (a, b, c, d and e), corresponding to the splitting of the EPR signal observed at g// by the interaction with the nuclear spin of each of the two naturally occurring copper isotopes.

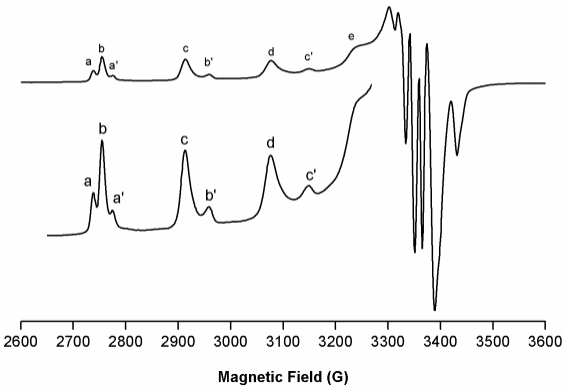

Figure 6: EPR spectrum of the complex Cu(hexylmpp)$_2$ in methanol registered at 100K.

The interaction of the unpaired electron with isotope ^{65}Cu originates lines a, c, d and e, while interaction with the most abundant ^{63}Cu isotope results in the appearance of lines b, c, d and e, as exemplified in Figure 6. The additional set of bands (a', b', c') is indicative of the presence in solution of an additional copper(II) species. The results described here are similar to those reported by Porte and co-workers[39] for copper(II) complexes with an O_4 coordination sphere provided by several types of ligands and obtained in chloroform and chloroform-toluene glasses. The authors have identified species represented by lines (a, b, c, d and e) as copper complexes whose electronic distribution is sensibly perturbed by interaction with neighbouring solvent molecules and species represented by lines (a', b', c') as copper(II) complexes for which this perturbation is not felt.

We agree that solvated and non-solvated copper(II) species are likely to be present in solution but we believe that in order to fully characterize all the species and distinguish between lines corresponding to copper isotopes or to solvated species, there is a need to isolate the "pure EPR signals" thus meaning to characterize EPR signals due to each individual species. In order to fulfil that objective we selected one compound and recorded EPR spectra in a variety of pure solvents (methanol, dimethylsulfoxide, dichloromethane) and their 50% (V:V) mixtures with toluene. The use of toluene provides formation of very good glasses and for that reason significantly improves spectral resolution.

EPR spectra of solvated and non-solvated species were obtained for compound 8 in methanol-toluene and dichloromethane-toluene glasses. Since the complex is not soluble in toluene, the addition of the latter solvent to MeOH, in which equilibrium between solvated and non-solvated species is present, favours the formation of the solvated species.

Dalton Transactions Accepted Manuscript

Experimental spectra together with their computer simulations are shown in Figure 7.

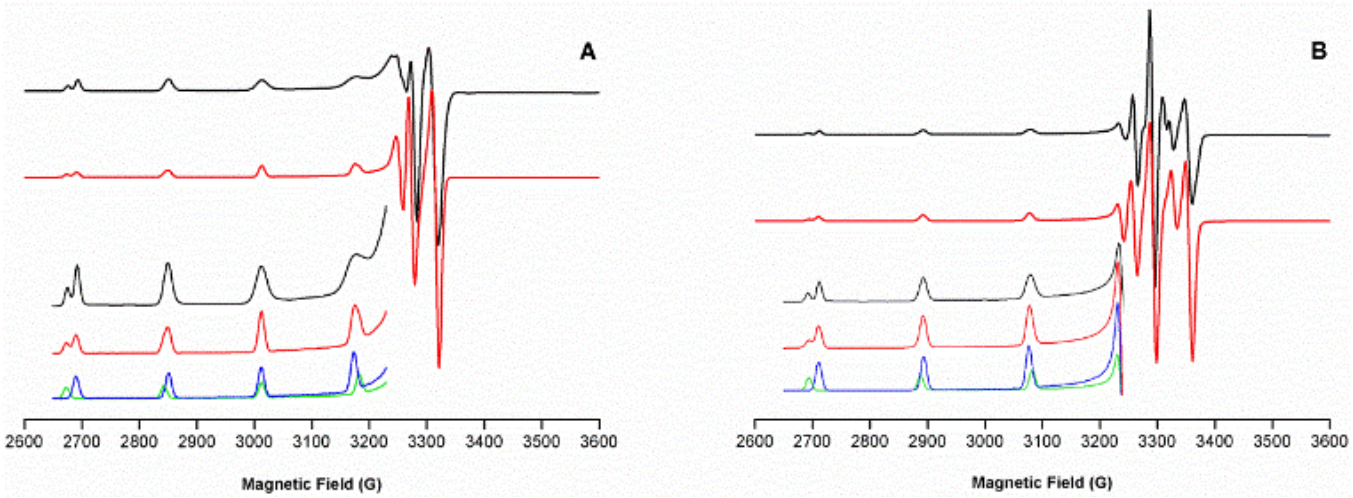

Figure 7: EPR spectra of Cu(hexylmpp)$_2$ in methanol-toluene (A) and in dichloromethane-toluene (B). Experimental (black line); Computer simulation (red line); Isotope components (green and blue lines).

Evidence for the presence of two copper isotopes is given by the fact that the best fit for spectra simulation was obtained considering the sum of two copper(II) signals with relative intensities that reproduce the isotopic abundance. The Spin-Hamiltonian parameters obtained from computer simulation for the two copper(II) species considering the symmetry and axis assignment previously described for this type of complexes are given in Table 5.[35-38]

Table 5: Spin-Hamiltonian parameters of the copper(II) species. The values of the components of the hyperfine tensor are in 10^{-4} cm^{-1}

	Copper(II) Solvated species		Copper(II) non-solvated species	
	^{63}Cu	^{65}Cu	^{63}Cu	^{65}Cu
g^{zz}	2.302	2.305	2.262	2.262
g^{yy}	2.061	2.064	2.064	2.064
g^{xx}	2.061	2.064	2.056	2.056
A^{zz}	171.0	181.0	193.0	205.0
A^{yy}	20.0	10.0	28.0	24.0
A^{xx}	20.0	10.0	28.0	24.0

The values of the components of the g and A tensors allow clear discrimination between solvated and non-solvated species. The spectrum with a larger g_{zz} value (2.30) and smaller A_{zz} values is due to the solvated species and the spectrum with a smaller g_{zz} value (2.26) and larger A_{zz} values is due to the non-solvated species. This assignement is in agreement with the interpretation of Porte *et al.*[39] that considers that the interaction with the solvent molecules does not result in molecular orbital mixing, and it can be better described in terms of the energy of the orbitals in the copper(II) chelates being altered by two electric dipoles orientated towards the axial direction of the complex. Based in this change in the energy of the molecular orbitals of the copper complexes, an increase in the g-tensor and a decrease in the hyperfine tensor, A, are predicted for the solvated species.

The two species may be further discriminated by the number of lines and shape of the spectra in the high field region. The best spectral fit for the species with g_{zz} = 2.26 reveals higher anisotropy, with $g_{xx} \neq g_{yy}$, resulting in a larger number of lines in the g⊥ region; in contrast, for the species with g_{zz} = 2.30 the values of g_{xx} and g_{yy} are identical and the spectrum is characterized by two sharp predominant lines in the high field region (Figure 7). The observation of such a difference in the high field region has not been discussed by Porte,[39] but we consider that they are very relevant and useful to visually distinguish signals due to different species since the lines are much more intense and quite sharp.

Simulation of complex spectra, such as that shown in Figure 6, where the two sets of lines appear (a and a'), was achieved by combining the simulation models of individual species as illustrated in Figure 8.

The specificity of solvent interactions associated with Cu(II) complexes and its reflection in the variation of the corresponding Spin-Hamiltonian parameters makes EPR an excellent tool to provide insight into the solvation of copper complexes, namely Cu(II) complexes derived from 3,4-HPO ligands, which we intend to use either to deliver copper to, or remove it from, living organisms.

In order to further explore this finding, a series of EPR spectra was obtained for preparations of compounds 5, 7 and 8,

Dalton Transactions Accepted Manuscript

This journal is © The Royal Society of Chemistry 2012

representative of 3 different hydro-lipophilic balances, in a variety of pure solvents (methanol, dimethylsulfoxide, dichloromethane) and their 50% (V:V) mixtures with toluene. Regarding the potential biological application of the ligands and

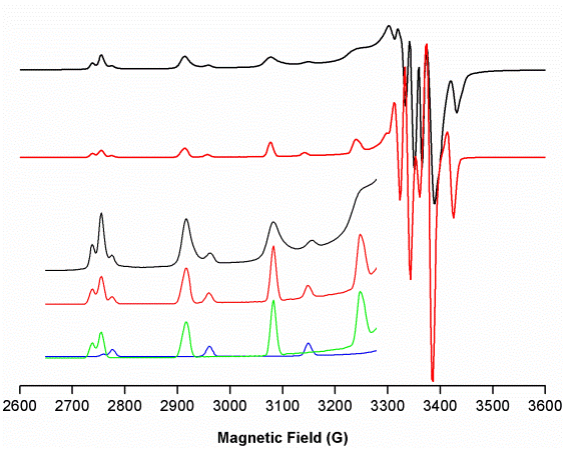

Figure 8: Computer simulation (red line) of the EPR spectrum of Cu(hexylmpp)$_2$ in methanol (black line); Isotope components (green and blue lines).

complexes and to gain insight into partition properties in water/membrane interfaces, EPR spectra were also obtained in wet-octanol, an aqueous solution buffered at pH = 7.4 and liposome suspensions. The results obtained are summarized in Table 6 in which we distinguish the two EPR signals by its g_{zz} values and indicate the predominance of each of the signals by a colour grade.

Analysis of the trends in Table 6 shows that the predominance of either the solvated (g_{zz} = 2.30) or non-solvated (g_{zz} = 2.26) species in solution is indicative of the lipophilicity of the complex and of its ability to interact with the solvent.

Comparison of the spectra obtained in aqueous buffer (10 mM MOPS pH = 7.4) and water-saturated octanol for compounds 5, 7 and 8, clearly shows that EPR can be used to characterize partition of the compounds into lipophilic media. Subsequently, EPR has been used to evaluate the distribution of the three copper complexes in a liposome suspension, as a means to mimicking their interaction with biological membranes.

The results obtained in liposome suspensions are shown in Figure 9 for the three compounds studied. Each spectrum is superimposed with the characteristic signal of the solvated or non-solvated species. From these results the importance of the lines in the high field region of the spectrum to identify the species present is clear. From the spectrum of the compound Cu(heepp)$_2$ it is possible to infer that it is in the water phase while for Cu(depp)$_2$ the spectrum exhibits in the high field region a feature that could be assigned to the presence of trace amounts of the non-solvated species. Contrastingly, the spectrum of Cu(hexylmpp)$_2$ is clearly superimposable on the pure g_{zz} = 2.26 signal thus indicating that the compound is located in the lipid phase.

Table 6: Summary of the type of copper(II) signal/signals observed in the different solvent mixtures. The signals are denoted by

Complex	**Cu(heepp)$_2$**		**Cu(depp)$_2$**		**Cu(hexyl)$_2$**	
g_{zz} value	**g_{zz} = 2.30**	**g_{zz} = 2.26**	**g_{zz} = 2.30**	**g_{zz} = 2.26**	**g_{zz} = 2.30**	**g_{zz} = 2.26**
CH_2Cl_2	not soluble	not soluble		+++		+++
MeOH	+++	++	+++	++	+++	++
DMSO	+++	++	+++	++	not soluble	not soluble
CH_2Cl_2_Tol	not soluble	not soluble		+++		+++
DMSO_Tol	++	++	++	++	not soluble	not soluble
MeOH_Tol	+++		+++		+++	
Octanol _water_sat	++	+++		+++		+++
Buffer pH=7.4	+++		+++		not soluble	not soluble
Liposome suspension	+++		+++	++		+++

their g_{zz} value and the predominance of each signal is indicated with the symbols (+++; ++;).

Dalton Transactions Accepted Manuscript

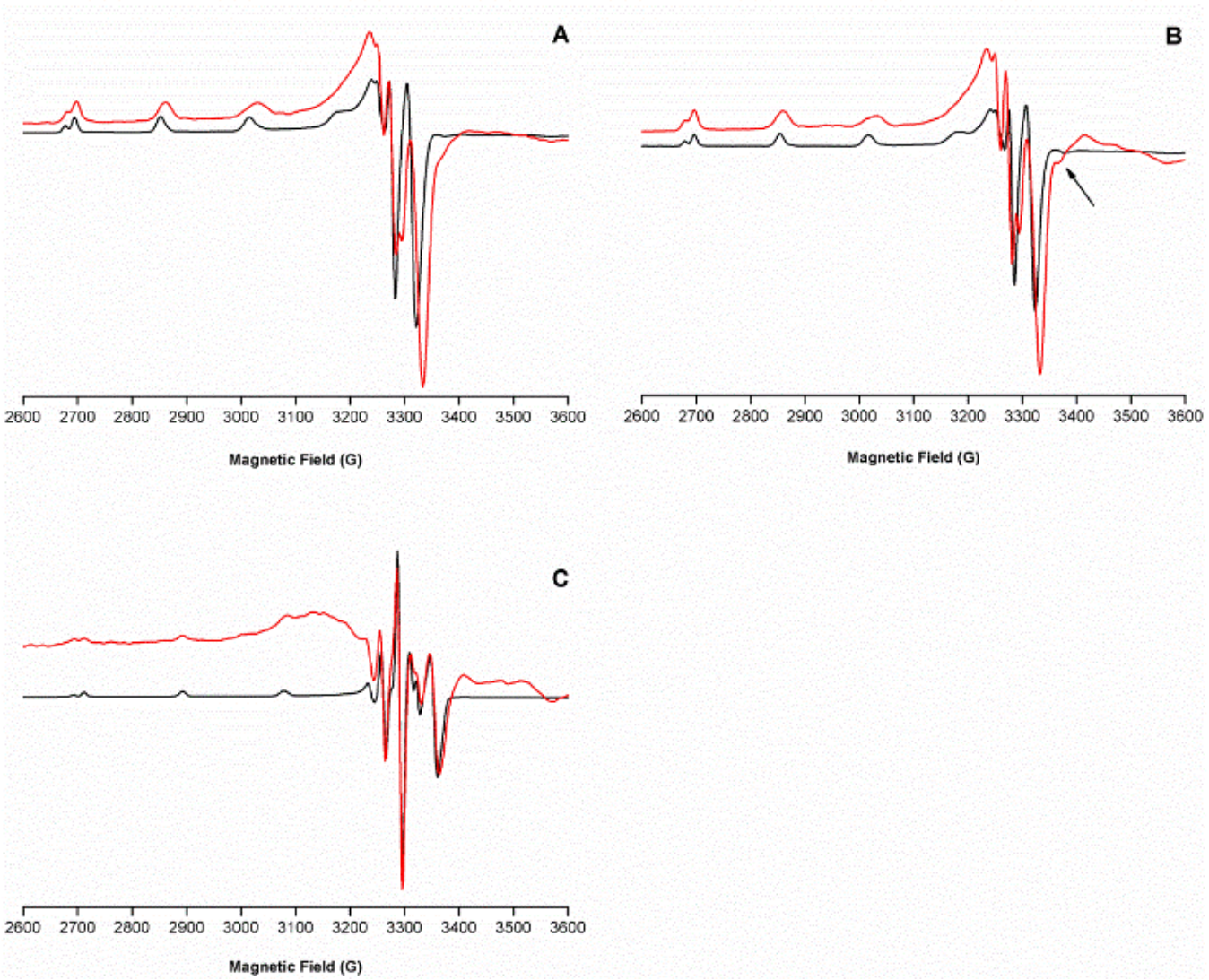

Figure 9: A) EPR spectra of $Cu(heepp)_2$ in DMPC (red line) and methanol-toluene (black line). B) EPR spectra of $Cu(depp)_2$ in DMPC (red line) and methanol-toluene (black line). C) EPR spectra of $Cu(hexylmpp)_2$ in DMPC (red line) and dichloromethane-toluene (black line).

Conclusions

Considering the results obtained in the present work we are confident that EPR spectroscopy can be used to estimate the location and partition properties of 3,4-HPO copper(II) complexes and that it also gives indirect information about the ligands and for other EPR-silent complexes. Evaluation of the partition properties in liposome suspensions is accepted to be much more realistic than octanol-water partition coefficients and the present results corroborate this idea. We intend to improve the experimental conditions in order to establish a methodology to calculate partition constants from EPR spectra obtained in liposome suspensions.

Based on the results obtained with the 3,4-HPO copper(II) complexes we believe that EPR is also a promising tool to evaluate the partition of Cu(II) complexes into biological membranes. Future studies of copper(II) complexes with different ligands will assess whether the methodology can be extended to other types of complex~~es~~.

Acknowledgements

This work received financial support from the European Union (FEDER funds through COMPETE) and National Funds (FCT, Fundação para a Ciência e Tecnologia) through project Pest-C/EQB/LA0006/2011. The Bruker Avance II 400 spectrometer is part of the National NMR network and was purchased under the framework of the National Programme for Scientific Re-equipment, contract REDE/1517/RMN/2005, with funds from POCI 2010 (FEDER) and (FCT). The Bruker ELEXYS EPR

Dalton Transactions Accepted Manuscript

This journal is © The Royal Society of Chemistry 2012

spectrometer was purchased under the framework of QREN, through project NORTE-07-0162-FEDER-000048. To all financing sources the authors are greatly indebted.

References

1. Burgess, J.; Rangel, M., Hydroxypyranones, hydroxypyridinones, and their complexes. In *Advances in Inorganic Chemistry, Vol 60*, van Eldik, R., Ed. 2008; Vol. 60, pp 167-243.
2. Crans, D. C.; Smee, J. J.; Gaidamauskas, E.; Yang, L. Q., *Chemical Reviews* 2004, *104*, 849-902.
3. Fernandes, S. S.; Nunes, A.; Gomes, A. R.; de Castro, B.; Hider, R. C.; Rangel, M.; Appelberg, R.; Gomes, M. S., *Microbes and Infection* 2010, *12*, 287-294.
4. Ma, Y.; Zhou, T.; Kong, X.; Hider, R. C., *Current Medicinal Chemistry* 2012, *19*, 2816-2827.
5. Moniz, T.; Amorim, M. J.; Ferreira, R.; Nunes, A.; Silva, A.; Queiros, C.; Leite, A.; Garneiro, P.; Sarmento, B.; Remiao, F.; Yoshikawa, Y.; Sakurai, H.; Rangel, M., *Journal of Inorganic Biochemistry* 2011, *105*, 1675-1682.
6. Moniz, T.; Nunes, A.; Silva, A. M. G.; Queiros, C.; Ivanova, G.; Gomes, M. S.; Rangel, M., *Journal of Inorganic Biochemistry* 2013, *121*, 156-166.
7. Nunes, A.; Podinovskaia, M.; Leite, A.; Gameiro, P.; Zhou, T.; Ma, Y. M.; Kong, X. L.; Schaible, U. E.; Hider, R. C.; Rangel, M., *Journal of Biological Inorganic Chemistry* 2010, *15*, 861-877.
8. Sakurai, H., *Expert Opinion on Drug Discovery* 2007, *2*, 873-887.
9. Santos, M. A.; Marques, S. M.; Chaves, S., *Coordination Chemistry Reviews* 2012, *256*, 240-259.
10. Thompson, K. H.; Orvig, C., *Journal of Inorganic Biochemistry* 2006, *100*, 1925-1935.
11. Bush, A. I., *Trends in Neurosciences* 2003, *26*, 207-214.
12. Crisponi, G.; Nurchi, V. M.; Fanni, D.; Gerosa, C.; Nemolato, S.; Faa, G., *Coordination Chemistry Reviews* 2010, *254*, 876-889.
13. Drago, D.; Bettella, M.; Bolognin, S.; Cendron, L.; Scancar, J.; Milacic, R.; Ricchelli, F.; Casini, A.; Messori, L.; Tognon, G.; Zatta, P., *International Journal of Biochemistry & Cell Biology* 2008, *40*, 731-746.
14. Lovell, M. A.; Robertson, J. D.; Teesdale, W. J.; Campbell, J. L.; Markesbery, W. R., *Journal of the Neurological Sciences* 1998, *158*, 47-52.
15. Yasumatsu, N.; Yoshikawa, Y.; Adachi, Y.; Sakurai, H., *Bioorganic & Medicinal Chemistry* 2007, *15*, 4917-4922.
16. Queiros, C.; Amorim, M. J.; Leite, A.; Ferreira, M.; Gameiro, P.; de Castro, B.; Biernacki, K.; Magalhaes, A.; Burgess, J.; Rangel, M., *European Journal of Inorganic Chemistry* 2011, 131-140.
17. Gerard, C., *Bulletin de la Societe Chimique de France Partie I-Physicochimie des Systemes Liquides Electrochimie Catalyse Genie Chimique* 1979, I451-I456.
18. Kottke, T.; Stalke, D., *Journal of Applied Crystallography* 1993, *26*, 615-619.
19. APEX2, *Data Collection Software Version 2.1-RC13, Bruker AXS, Delft, The Netherlands* 2006.
20. Cryopad, *Remote monitoring and control, Version 1.451, Oxford Cryosystems, Oxford, United Kingdom* 2006.
21. SAINT+, *Data Integration Engine v. 7.23a* ©1997-2005, Bruker AXS, Madison, Wisconsin, USA.
22. Sheldrick, G. M., SADABS v.2.01, Bruker/Siemens Area Detector Absorption Correction Program 1998, Bruker AXS, Madison, Wisconsin, USA.
23. Sheldrick, G. M., SHELXS-97, Program for Crystal Structure Solution, University of Göttingen 1997.
24. Sheldrick, G. M., Acta Cryst. A 2008, 64, 112-122.
25. Gran, G., Analyst 1952, 77, 661-671.
26. Gans, P.; Sabatini, A.; Vacca, A., Talanta 1996, 43, 1739-1753.
27. Albert, A.; Sergeant, E. P., The Determination of Ionization Constants. 2nd ed.; Chapman & Hall: London, 1971.
28. Allen, F. H., Acta Cryst. B 2002, 58, 380-388.
29. Allen, F. H.; Motherwell, W. D. S., Acta Cryst. B 2002, 58, 407-422.
30. El-Jammal, A.; Howell, P. L.; Turner, M. A.; Li, N.; Templeton, D. M., Journal of Medicinal Chemistry 1994, 37, 461-466.
31. Green, D. E.; Bowen, M. L.; Scott, L. E.; Storr, T.; Merkel, M.; Bohmerle, K.; Thompson, K. H.; Patrick, B. O.; Schugar, H. J.; Orvig, C., Dalton Transactions 2010, 39, 1604-1615.
32. Scott, L. E.; Page, B. D. G.; Patrick, B. O.; Orvig, C., Dalton Transactions 2008, 6364-6367.
33. Scott, L. E.; Telpoukhovskaia, M.; Rodriguez-Rodriguez, C.; Merkel, M.; Bowen, M. L.; Page, B. D. G.; Green, D. E.; Storr, T.; Thomas, F.; Allen, D. D.; Lockman, P. R.; Patrick, B. O.; Adam, M. J.; Orvig, C., Chemical Science 2011, 2, 642-648.
34. Rangel, M.; Leite, A.; Amorim, M. J.; Garribba, E.; Micera, G.; Lodyga-Chruscinska, E., Inorganic Chemistry 2006, 45, 8086-8097.
35. Calvo, R.; Passeggi, M. C. G.; Isaacson, R. A.; Okamura, M. Y.; Feher, G., Biophysical Journal 1990, 58, 149-165.
36. Chow, C.; Chang, K.; Willett, R. D., Journal of Chemical Physics 1973, 59, 2629-2640.
37. Maki, A. H.; McGarvey, B. R., Journal of Chemical Physics 1958, 29, 31-34.
38. Solomon, E. I.; Baldwin, M. J.; Lowery, M. D., Chemical Reviews 1992, 92, 521-542.
39. Antosik, S.; Brown, N. M. D.; McConnel.Aa; Porte, A. L., Journal of the Chemical Society A - Inorganic Physical Theoretical 1969, 545-550.

Notes and references

[a] *REQUIMTE*, Instituto de Ciências Biomédicas de Abel Salazar, Universidade do Porto, Portugal.
[b] *REQUIMTE*, Departamento de Química e Bioquímica, Faculdade de Ciências, Universidade do Porto, Portugal.
[c] Department of Chemistry, University of Leicester, Leicester, LE1 7RH, UK.

Dalton Transactions Accepted Manuscript

Graphical Abstract

In view of the present results we put forward the use of EPR spectroscopy to assess the affinity of *bis*-(3-hydroxy-4-pyridinonato) copper (II) complexes for a hydrophobic environment and also to obtain indirect information about the lipophilicity of the ligands and similar EPR silent complexes.

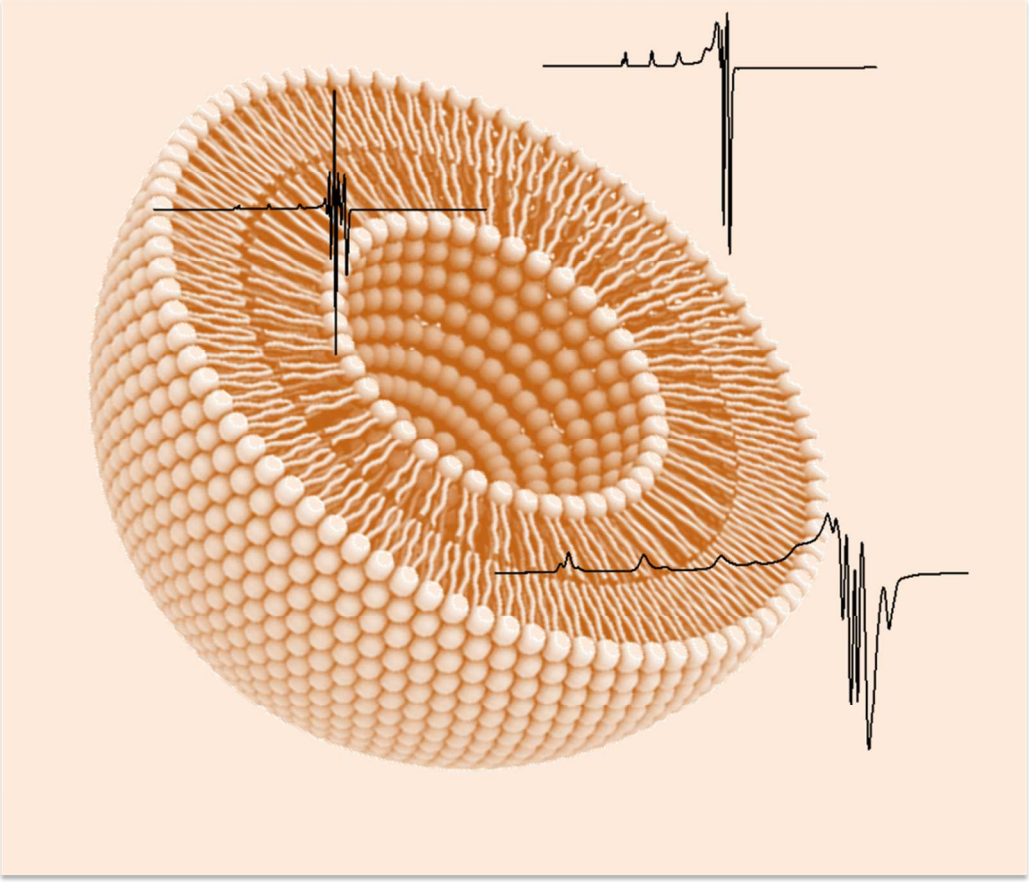

Dalton Transactions Accepted Manuscript